Zitierweise: *Angew. Chem. Int. Ed.* **2023**, *62*, e202305460
doi.org/10.1002/anie.202305460

Carbon Nanodots

Chiral Carbon Nanodots Can Act as Molecular Catalysts in Chemical and Photochemical Reactions

Beatrice Bartolomei[+], *Vasco Corti*[+], *and Maurizio Prato**

Dedicated to Professor Robert Deschenaux on the occasion of his 70th birthday

Abstract: In this work, a microwave synthesis followed by a simple purification process produces a new type of chiral Carbon Nanodots (CNDs). These CNDs are soluble in organic solvents, exhibit amino groups on their surface and display interesting absorption and emission properties along with mirror image profiles in the electronic circular dichroism spectrum. All these features set the stage for CNDs to act as multifunctional catalytic platforms, able to promote diverse chemical transformations. In particular, the outer shell composition of CNDs was instrumental to carry out organocatalytic reactions in an enantioselective fashion. In addition, the redox and light-absorbing properties of the material are suitable to drive photochemical processes. Finally, the photoredox and organocatalytic activations of CNDs were exploited at the same time to promote a cross-dehydrogenative coupling. This work demonstrates that CNDs can be used as catalysts to promote multiple reactivities, previously considered exclusive domain of molecular catalysts.

Introduction

Carbon Nanodots (CNDs) are an emerging class of nanoparticles that present many interesting physicochemical properties, such as tunable photoluminescence, dispersibility and low toxicity.[1,2] They are defined by characteristic sizes below 10 nm, a carbon-based core covered by surface functional groups, such as carboxylic acids, alcohols, or amines. In recent times, the commonly employed synthetic strategy for the preparation of these materials has relied on the solvothermal treatment of small organic molecules. Indeed, the appropriate selection of starting materials, doping agents, and synthetic conditions affords CNDs with tailored structural and optical properties.[3–5] Among other possible applications, CNDs can be considered as a new generation of nano-catalysts. Indeed, recent literature examples demonstrated the possibility to use CNDs for the preparation of valuable organic compounds under mild operating conditions by means of classical dark or light-driven reactivities.[6–11] Despite recent encouraging advancements in this research field, the use of CNDs as nano-organocatalysts for the stereoselective preparation of chiral compounds remains an elusive goal. This can possibly be related to the challenging conditions used in the preparation of chiral CNDs. Indeed, the high temperatures required for the synthesis of the carbon nanoparticles may lead to the loss of the chiral information present in the starting materials. However, recent literature showed how, in some cases, the synthesis of chiral CNDs can be accomplished using chiral molecular precursors, such as cysteine, glucose or tartaric acid, among others.[12] A different synthetic approach is based on the addition of a chiral "doping" agent to the carbon source during the preparation step.[13,14] The widespread recurrence in nature of enantiomerically pure molecular motifs provides an appealing chiral pool for developing the synthesis of new optically active CNDs featuring hitherto undisclosed properties. For example, our group reported the synthesis of chiral CNDs using *L*-arginine and (*S,S*)-1,2-cyclohexanediamine as precursors to obtain a material that was able to promote the aldol addition of acetone to isatine.[7] Despite the poor enantioselectivity induced during the reaction, this example demonstrated that the chirality of the surface amino groups of the CNDs can be partially transferred to the product. Soon afterwards, Xu et al. applied proline-derived CNDs to promote the aldol addition of cyclohexanone and 4-NO_2-benzaldehyde to obtain the corresponding product in 98 % yield, 96 % d.r., and 71 % ee.[15] It should be underlined that, to our knowledge, these are the only two examples in the literature that report the use of CNDs in asymmetric catalysis.

The use of doping agents for the preparation of CNDs offers the possibility to tune not only the surface composi-

[*] B. Bartolomei,[+] Dr. V. Corti,[+] Prof. M. Prato
Department of Chemical and Pharmaceutical Sciences, INSTM UdR Trieste, University of Trieste
via Licio Giorgieri 1, 34127 Trieste (Italy)
E-mail: prato@units.it
Prof. M. Prato
Center for Cooperative Research in Biomaterials (CIC biomaGUNE), Basque Research and Technology Alliance (BRTA)
Paseo de Miramón 194, 20014 Donostia San Sebastián (Spain)
Prof. M. Prato
Basque Fdn Sci, Ikerbasque
48013 Bilbao (Spain)
[+] These authors contributed equally to this work.

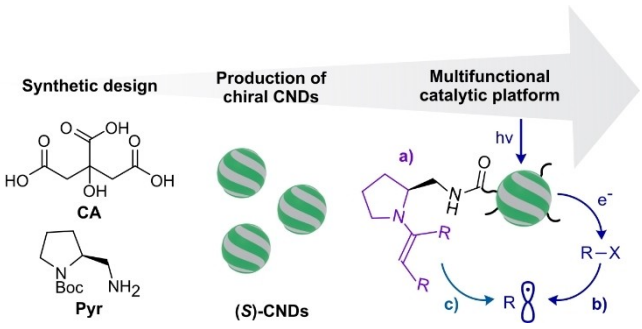

Figure 1. General Scheme for the synthesis of **(*S*)-CNDs** and their use in a) organocatalytic, b) photoredox and c) organophotoredox processes.

tion of the nanoparticles, but also the redox and photophysical properties of the material, enabling the use of CNDs as promoters of photochemical processes.[3,16,17] In particular, it is reported that nitrogen doped CNDs are able to drive the photochemical addition of easily reducible radical precursors to unsaturated molecules or cross-coupling reactions.[6,10] A still unexplored strategy in literature is the combination of the organocatalytic activity of the CND surface with the photoredox properties of the nanoparticles, which can open new types of reactivity. In order to explore the versatility of carbon nanoparticles as multifunctional synthetic platforms, we envisioned that, by selecting an appropriate chiral "doping" agent, it could be possible to obtain a new chiral nanoparticle that is also photochemically active. This new type of chiral CNDs could therefore be used as nano-organocatalysts to promote stereoselective reactions as well as photochemical processes. Finally, these two different activation modes, provided by the same CNDs, could be combined to promote more complex reactivities.

In this work, a new type of chiral CNDs was synthesized employing citric acid (**CA**) as carbon source, in combination with (*S*)-2-(aminomethyl)-1-Boc-pyrrolidine (**Pyr**) (or its (*R*)-enantiomer) as chiral dopant (Figure 1). It was anticipated that the configurational stability of this amine would prevent the loss of the stereochemical information during the synthetic process, resulting in the production of chiral nanoparticles. Furthermore, the pyrrolidine core has been recognized to be a privileged scaffold for the development of a wide variety of chiral organocatalysts.[18]

The newly synthesized CNDs present mirror image profiles in the electronic circular dichroism spectrum (Figure 2e). The presence of secondary amino groups on the surface enabled the activation of carbonyl compounds via enamine intermediates, mimicking the typical activity of molecular aminocatalysts to obtain enantioenriched products.[19–22] Furthermore, the intrinsic photophysical and redox properties of the synthesized nanoparticles were leveraged to drive photochemical transformations.[23,24] Finally, it was possible to combine the activation of the surface amino groups with the photochemical activity of CNDs to promote one type of organophotoredox reaction (Figure 1).[25]

Results and Discussion

The new chiral CNDs were prepared via microwave-assisted synthesis, in which a heterogeneous aqueous dispersion of **CA** and **Pyr** was heated to 240 °C for 180 seconds. After the synthesis, the crude product presented good solubility in organic solvents, such as chloroform and methanol. The purification of the material was carried out performing a chloroform/water extraction followed by precipitation with diethyl ether, obtaining a brownish solid defined as **(*S*)-CNDs** or **(*R*)-CNDs** depending on which enantiomer of the chiral amine was used during the synthesis (see Figure S1 of the SI).

The effective purification of the final CNDs from the starting materials or molecular species was ascertained employing nuclear magnetic resonance (NMR), which showed only broad aliphatic signals, compatible with the presence of carbon nanoparticles (Figure 2a). The lack of sharp molecular signals in the ^{1}H NMR spectrum indicates the efficient purification of the material from residual molecules or oligomers that can be formed during the thermal treatment.[26,27] Moreover, the Boc signal of the starting **Pyr** (methyl groups at 1.5 ppm, Figure S2), is not observed in the spectrum of CNDs, confirming the amine deprotection during the synthetic process, as expected based on previous literature.[28,29] Atomic force microscopy (AFM) measurements reveal particles with an average size of 2.7 ± 0.4 nm (Figure 2c, Figure S3). The UV/Vis absorption spectrum of CNDs presents a broad band centered at around 340 nm (Figure 2d). The emission spectra show an excitation wavelength-dependent profile and the fluorescence peak shifts from 460 to 570 nm when the excitation wavelength changes from 340 to 500 nm. Furthermore, the photolumi-

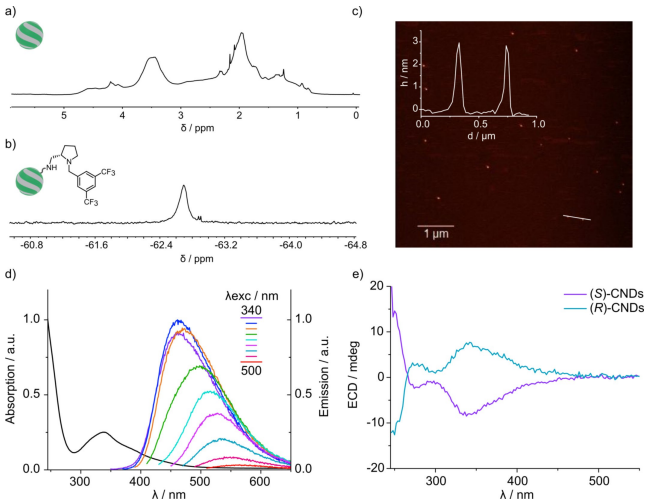

Figure 2. Characterization of **(*S*)-CNDs**. a) ^{1}H NMR spectrum ($CDCl_3$, 500 MHz, rt). b) ^{19}F NMR spectrum of **(*S*)-CNDs** after the reductive amination for the quantification of the surface amino groups ($CDCl_3$, 400 MHz, rt). c) Tapping mode AFM of sample drop-cast on a mica substrate from a methanol solution; inset is the height profile along the white line. d) Absorption and emission spectra recorded at different excitation wavelengths. e) ECD spectra of **(*S*)-** and **(*R*)-CNDs**. All the optical spectra were recorded in chloroform.

nescence quantum yield (PLQY) was determined to be around 30 % over the entire range of excitation (Figure S4). Then, long average fluorescence lifetimes were measured resulting in 8 ns (double-exponential fit showed a short $\tau_1 =$ 1.1 ns and a long $\tau_2 = 11.6$ ns component Figure S5 and Table S1). To assess the chirality of the material, electronic circular dichroism (ECD) was employed showing that **(*S*)-CNDs** and **(*R*)-CNDs** display mirror images of the ECD spectrum characterized by a maximum at 340 nm, paralleling the UV/Vis absorption spectrum (Figure 2e). Insights into the structure and composition of (*S*)-CNDs were obtained through FT-IR spectroscopy and X-ray photoelectron spectroscopy (XPS). The FT-IR spectrum (Figure S6) shows a broad peak centered at 3440 cm^{-1} that can be associated to O–H/N–H bonds, while the peaks at 2950 and 2870 cm^{-1} can be assigned to C–H bond stretching vibrations. Furthermore, compared to the starting materials, two new peaks around 1630 and 1535 cm^{-1} can be observed in the CNDs spectrum which are compatible with the C=O and C–N stretching of amide groups.[30] From the full-scan XPS spectrum of (*S*)-CNDs (Figure S7) C, O, N were detected (C1s at 284.5 eV, O1s at 531.4 eV, and N1s at 399.7 eV). The atomic percentage for C, O, N are as follows: 78.8, 13.4, 7.8, respectively. Deconvolution of C1s peak indicates that more than 50 % of C participate in C–C/C=C bonds and reveals the presence of both C–O/C–N and C=O bonds, in agreement with the FT-IR interpretation.[31]

To investigate the potential use of this material as versatile nano-catalyst, the quantification of reactive sites and evaluation of redox properties is essential. To gain information about the presence and concentration of reactive amines on the surface of the nanoparticles, a reductive amination reaction was carried out using 3,5-bis(trifluoromethyl)benzaldehyde in the presence of $NaCNBH_3$. This transformation allowed the quantification of the reactive surface amines by means of ^{19}F NMR, which resulted to be around 300 µmol/g (Figure 2b). The electrochemical properties of **(*S*)-CNDs** were investigated through cyclic voltammetry in dichloromethane, which showed an irreversible reduction peak at $E = -1.3$ V and an irreversible oxidation peak at $E = +1.1$ V (vs. SCE, Figure S9).

The amines present on the surface of **(*S*)-CNDs** can be used to activate α-enolizable carbonyl compounds through the formation of enamine intermediates. Indeed, these species show an improved nucleophilic character, compared to the corresponding enol, and have been widely used to promote organocatalyzed transformations (HOMO-rising activation).[32]

Initially, in order to test the catalytic activity, as well as the recyclability of the new material, **(*S*)-CNDs** were employed in the direct organocatalytic aldol reaction between cyclohexanone **1a** and 4-NO_2-benzaldehyde **2** in 1,2-dichloroethane (1,2-DCE) with a sub-stoichiometric amount of benzoic acid (BzOH). The aldol adduct **3** was obtained in 81 % yield, 3:1 d.r. and 37 % and 17 % ee respectively at room temperature, demonstrating that the stereochemical information of the nanomaterial surface can be transferred to the final products to obtain a partial enantioinduction (Figure 3a). Furthermore, **(*S*)-CNDs** could

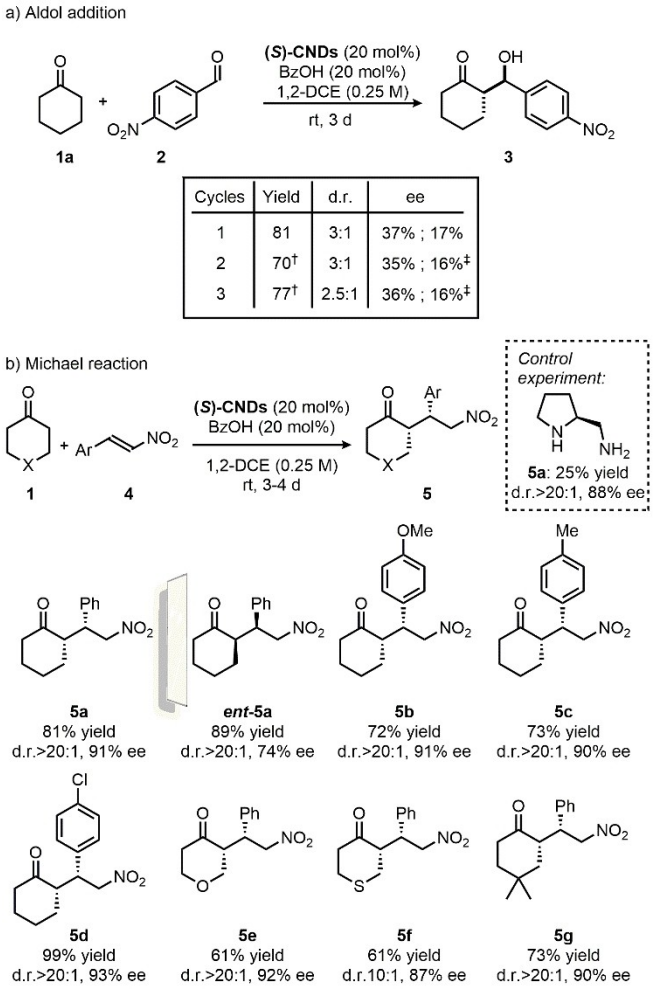

Figure 3. a) **(*S*)-CNDs**-catalyzed aldol reaction between cyclohexanone and 4-NO_2-benzaldehyde and recyclability tests. Conditions: **1a** (0.25 mmol), **2** (0.05 mmol), BzOH (20 mol%), **(*S*)-CNDs** (38 mg), 1,2-DCE (0.25 M), 3 d. †The yield was determined by ^1H NMR analysis on the crude mixture using 1,3,5-trimethoxybenzene as internal standard. ‡The enantiomeric excess was evaluated on the crude mixture. b) **(*S*)-CNDs**-catalyzed Michael addition of cyclohexanones to nitroalkenes. Conditions: **1** (0.25 mmol), **4** (0.05 mmol), BzOH (20 mol%), **(*S*)-CNDs** (38 mg), 1,2-DCE (0.25 M), 3 d (for entry 5a) – 4 d (for entries *ent*-5a, 5b-g). All the reactions were performed on a 0.05 mmol scale using 38 mg of **(*S*)-CNDs**, corresponding to 20 mol% of surface pyrrolidines based on the amine quantification performed through reductive amination.

be recovered after the catalytic reaction performing a simple precipitation of the crude mixture with diethyl ether. The recovered nanoparticles could be reused, up to three cycles, in subsequent catalytic reactions, providing comparable performances in terms of reaction yield and stereoselectivity. These experiments show that catalyst deactivation does not seem to occur during the reaction, thus highlighting the potential use of **(*S*)-CNDs** as recyclable nano-organocatalysts.

The secondary amines on the surface of **(*S*)-CNDs**, probably linked to the CND structure by an amide bond, are therefore flanked to a hydrogen bond donor moiety and

resemble the structural motifs of various organocatalysts used to promote addition reactions of carbonyl compounds to nitroalkenes.[33] In particular, we tested **(*S*)-CNDs** in the enamine-mediated Michael addition of cyclohexanones to nitroolefines. Notably, the reaction between cyclohexanone **1a** and *trans*-β-nitrostyrene **4a**, in the presence of **(*S*)-CNDs**, afforded the corresponding Michael adduct **5a** in high yield and excellent diastereo- and enantioselectivity (81 % yield, >20:1 d.r. and 91 % ee) (Figure 3b). It was also confirmed that the enantiomeric material **(*R*)-CNDs** provided the enantiomeric form ***ent*-5a** in excellent yield and diastereoselectivity albeit in lower optical purity (89 % yield, >20:1 d.r. and 74 % ee). The reason for lower enantioselectivity in this case is not well understood and is the object of current investigations.

To prove the generality of this methodology, we tested a small library of nitroalkenes as well as cyclohexanone derivatives. While nitrostyrenes featuring an electron-donating group at the 4-position of the phenyl ring provided products **5b** and **5c** in comparable yields and excellent stereoselectivities (Figure 3b, 72 % yield, >20:1 d.r., 91 % ee and 73 % yield, >20:1 d.r. and 90 % ee, respectively), an electron-withdrawing group, such as a chlorine atom, proved beneficial, affording product **5d** in quantitative yield and slightly higher enantioselectivity (Figure 3b, 99 % yield, >20:1 d.r., 93 % ee). Then, we tested different cyclohexanone derivatives obtaining products **5e**–**5g**, possessing either a heteroatom or a *gem*-dimethyl moiety at the 4-position of the ring, in good yields, diastereo- and enantioselectivities (Figure 3b, 61–73 % yield, 10–20:1 d.r. and 87–92 % ee).

Finally, we carried out a control experiment performing the reaction between **1a** and **4a** under the same reaction conditions, but using (*S*)-2-(aminomethyl)pyrrolidine (no **(*S*)-CNDs**) as organocatalyst. The desired product **5a** was obtained in 25 % isolated yield, >20:1 d.r. and 88 % ee. This result highlights the beneficial incorporation of the starting amine in the **(*S*)-CNDs** scaffold resulting in improved catalytic performances. The absolute configuration of product **5a** was determined by comparison of its specific rotation with the one reported in literature and resulted in the (*S*,*R*) configuration (see Supporting Information). The absolute configuration of the other Michael adducts was assigned by analogy.

We next investigated the use of **(*S*)-CNDs** in the field of photochemical transformations. Indeed, **(*S*)-CNDs**, upon light absorption, can directly reach an electronically excited state (**(*S*)-CNDs***) that could trigger the formation of reactive radicals through a single-electron transfer (SET) process. To test the feasibility of our strategy, bromotrichloromethane ($BrCCl_3$) was selected as radical source and a series of Stern–Volmer quenching studies were performed (Figure S10). The emission spectrum of **(*S*)-CNDs** after excitation at $\lambda = 456$ nm was recorded and upon addition of $BrCCl_3$ an increasing quenching of the emission of **(*S*)-CNDs*** was observed. These photochemical studies suggest that the photo-induced SET from **(*S*)-CNDs*** to $BrCCl_3$ could be viable at ambient temperature, thus prompting the formation of radical species. The photochemical activity of **(*S*)-CNDs** was then evaluated by studying the reaction between $BrCCl_3$ **7a** and 5-hexenyl acetate **6a** under visible light irradiation with a Kessil lamp ($\lambda = 456$ nm). The photochemically generated radical intermediate could be trapped by the alkene to afford the corresponding atom transfer radical addition (ATRA) product **8a** in excellent yield (Figure 4a).

This process could be extended to a small variety of terminal alkenes bearing different functional groups and other radical sources, such as diethyl bromomalonate, obtaining the corresponding products in good yields (**8b**–**d**, 64–72 % yield). It is worth noting that these reactions were carried out with an **(*S*)-CNDs** loading as low as 6 mg for a 0.1 mmol scale reaction of limiting reagent. Interestingly, **(*S*)-CNDs** were able to promote an intermolecular cyclopropanation of α-bromo-β-ketoester **9** with the unactivated olefin **10**.[34] By slightly modifying the reaction conditions reported in the literature, **(*S*)-CNDs**, in the presence of $LiBF_4$ and 2,6-lutidine, were able to promote the reaction affording cyclopropane **11** in 35 % yield as a single diastereomer, under blue light irradiation (Figure 4b).

In recent years, the synergistic combination of photoredox catalysis with other catalytic systems has emerged as a powerful approach to discover novel reactivities otherwise unattainable.[35] A photocatalyst is used to generate reactive radical species in solution that can be intercepted with an organocatalytic intermediate. This synthetic strategy has been used, for example, in the cross-dehydrogenative coupling of aldehydes with xanthenes.[36,37]

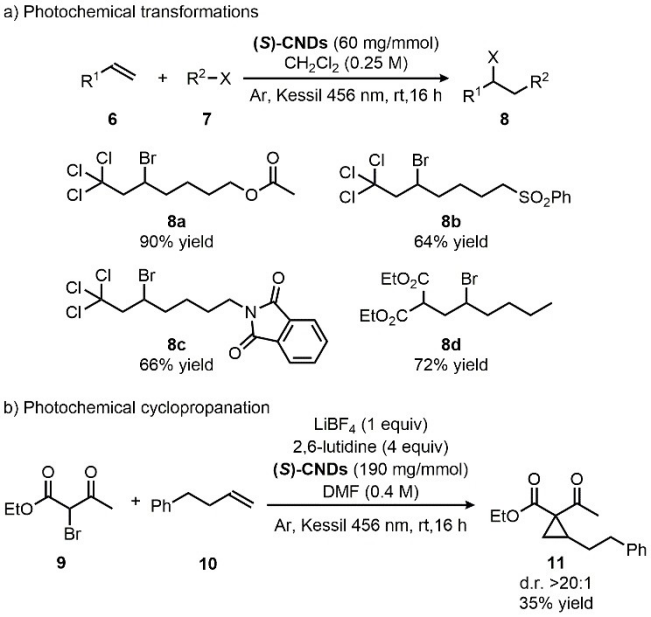

Figure 4. a) **(*S*)-CNDs** catalyzed ATRA reactions. Conditions: **6** (0.1 mmol), **7** (0.3 mmol), CH_2Cl_2 (0.25 M), **(*S*)-CNDs** (6 mg), Kessil lamp 456 nm, Ar, 16 h. b) **(*S*)-CNDs** catalyzed photocyclopropanation. Conditions: **9** (0.2 mmol), **10** (0.1 mmol), $LiBF_4$ (0.1 mmol), 2,6-lutidine (0.4 mmol), DMF (0.4 M), **(*S*)-CNDs** (19 mg), Kessil lamp 456 nm, Ar, 16 h.

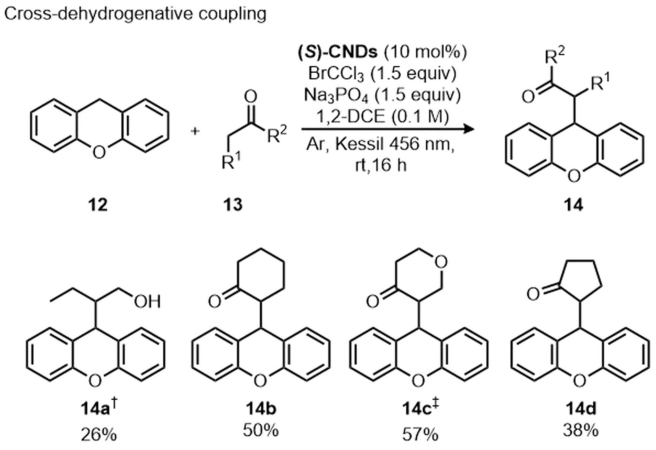

Figure 5. **(*S*)-CNDs**-catalyzed cross-dehydrogenative coupling. Conditions: **12** (0.05 mmol), **13** (0.15 mmol), $BrCCl_3$ (0.075 mmol), Na_3PO_4 (0.075 mmol), 1,2-DCE (0.1 M), **(*S*)-CNDs** (19 mg), Kessil lamp 456 nm, Ar, 16 h. All the reactions were performed using 19 mg of **(*S*)-CNDs**, corresponding to 10 mol% of surface pyrrolidines based on the amine quantification performed through reductive amination. †The crude mixture was diluted with MeOH (1 mL), cooled to 0 °C, treated with $NaBH_4$ (0.5 mmol) and stirred for 4 h allowing the reaction temperature to reach rt. ‡Reaction performed with 38 mg of **(*S*)-CNDs**.

In this methodology, the optimized combination of a metal-based photocatalyst and a chiral aminocatalyst was the key to obtain the direct functionalization of the inert C–H bond of xanthene. The ability of **(*S*)-CNDs** to both form enamine intermediates and to generate open-shell intermediates could be exploited to promote the same reaction combining the two catalytic systems into a single entity. To test the applicability of this strategy, xanthene **12** and butyraldehyde **13a** were treated with $BrCCl_3$ and Na_3PO_4 in the presence of **(*S*)-CNDs** under blue light irradiation. These reaction conditions provided the corresponding coupling product **14a** in 26 % yield as a racemic mixture (Figure 5). The lack of stereoinduction is probably due to the low degree of steric bulk of the surface amines that is therefore not able to discriminate the two prochiral faces of the enamine intermediate. However, **(*S*)-CNDs** allowed the use of cyclic ketones as carbonylic substrates. Indeed, products **14b**–**d** were isolated in yields ranging from 38 to 57 % (Figure 5). This organophotoredox strategy, which capitalizes on the two activation modes of **(*S*)-CNDs** in the ground and the excited states, can offer alternative opportunities for the design of new catalytic systems.

Conclusion

In summary, chiral CNDs were successfully synthesized employing a new type of chiral amine as doping agent and a green microwave assisted process. This strategy gives rise to chiral nanoparticles with excellent optical properties and with surface amino groups. The **(*S*)-CNDs** were used as recyclable organocatalysts to promote organic transformations affording enantioenriched products. Moreover, **(*S*)-CNDs** were able to photo-reduce radical precursors and promote photochemical transformations under mild conditions. Eventually, the organo- and photochemical properties of the material were combined to realize a cross-dehydrogenative coupling, allowing the replacement of metal photocatalysts generally used for this type of transformation. The presented results show the possibility to exploit diverse features of the same material to promote multiple reactivities, paving the way to use **(*S*)-CNDs** as a multifunctional synthetic platform.

Acknowledgements

M.P. is the AXA Chair for Bionanotechnology (2016–2026). The authors gratefully acknowledge the financial support from the European Research Council (ERC AdG-2019 n. 885323, e-DOTS), the Spanish Ministry of Economy and Competitiveness MINECO (project PID2019-108523RB-I00), the University of Trieste, INSTM, the Italian Ministry of Education MIUR (cofin Prot. 2017PBXPN4) and the Maria de Maeztu Units of Excellence Program from the Spanish State Research Agency (Grant No. MDM-2017-0720). The authors acknowledge the financial support of the University of Michigan College of Engineering and NSF grant #DMR-0420785 to BB, and technical support from the Michigan Center for Materials Characterization. We thank Dr. Alessandro Silvestri (University of Venezia) for XPS interpretation.

Conflict of Interest

The authors declare no conflict of interest.

Data Availability Statement

The data that support the findings of this study are available in the supplementary material of this article.

Keywords: Carbon Dots · Chirality · Nanocatalysis · Organocatalysis · Photocatalysis

[1] J. Liu, R. Li, B. Yang, *ACS Cent. Sci.* **2020**, *6*, 2179–2195.
[2] G. Ragazzon, A. Cadranel, E. V. Ushakova, Y. Wang, D. M. Guldi, A. L. Rogach, N. A. Kotov, M. Prato, *Chem* **2021**, *7*, 606–628.
[3] F. Arcudi, L. Đorđević, M. Prato, *Acc. Chem. Res.* **2019**, *52*, 2070–2079.
[4] L. Đorđević, F. Arcudi, M. Cacioppo, M. Prato, *Nat. Nanotechnol.* **2022**, *17*, 112–130.
[5] R. de Boëver, J. R. Town, X. Li, J. P. Claverie, *Chem. Eur. J.* **2022**, *28*, e202200748.
[6] C. Rosso, G. Filippini, M. Prato, *Chem. Eur. J.* **2019**, *25*, 16032–16036.
[7] G. Filippini, F. Amato, C. Rosso, G. Ragazzon, A. Vega-Peñaloza, X. Companyó, L. Dell'Amico, M. Bonchio, M. Prato, *Chem* **2020**, *6*, 3022–3037.

[8] C. Rosso, G. Filippini, M. Prato, *ACS Catal.* **2020**, *10*, 8090–8105.
[9] V. Corti, B. Bartolomei, M. Mamone, G. Gentile, M. Prato, G. Filippini, *Eur. J. Org. Chem.* **2022**, e202200879.
[10] Z. Zhao, B. Pieber, M. Delbianco, *ACS Catal.* **2022**, *12*, 13831–13837.
[11] G. Gentile, M. Mamone, C. Rosso, F. Amato, C. Lanfrit, G. Filippini, M. Prato, *ChemSusChem* **2023**, *16*, e202202399.
[12] A. Döring, E. Ushakova, A. L. Rogach, *Light-Sci. Appl.* **2022**, *11*, 75.
[13] L. Đorđević, F. Arcudi, A. D'Urso, M. Cacioppo, N. Micali, T. Bürgi, R. Purrello, M. Prato, *Nat. Commun.* **2018**, *9*, 3442.
[14] S. Di Noja, F. Amato, F. Zinna, L. Di Bari, G. Ragazzon, M. Prato, *Angew. Chem. Int. Ed.* **2022**, *61*, e202202397.
[15] S. Liu, Y. He, Y. Liu, S. Wang, Y. Jian, B. Li, C. Xu, *Chem. Commun.* **2021**, *57*, 3680–3683.
[16] B. C. M. Martindale, G. A. M. Hutton, C. A. Caputo, S. Prantl, R. Godin, J. R. Durrant, E. Reisner, *Angew. Chem. Int. Ed.* **2017**, *56*, 6459–6463.
[17] S. Miao, K. Liang, J. Zhu, B. Yang, D. Zhao, B. Kong, *Nano Today* **2020**, *33*, 100879.
[18] A. Vega-Peñaloza, S. Paria, M. Bonchio, L. Dell'Amico, X. Companyó, *ACS Catal.* **2019**, *9*, 6058–6072.
[19] S. Mukherjee, J. W. Yang, S. Hoffmann, B. List, *Chem. Rev.* **2007**, *107*, 5471–5569.
[20] P. Melchiorre, M. Marigo, A. Carlone, G. Bartoli, *Angew. Chem. Int. Ed.* **2008**, *47*, 6138–6171.
[21] S. Bertelsen, K. A. Jørgensen, *Chem. Soc. Rev.* **2009**, *38*, 2178–2189.
[22] B. S. Donslund, T. K. Johansen, P. H. Poulsen, K. S. Halskov, K. A. Jørgensen, *Angew. Chem. Int. Ed.* **2015**, *54*, 13860–13874.
[23] M. H. Shaw, J. Twilton, D. W. C. MacMillan, *J. Org. Chem.* **2016**, *81*, 6898–6926.
[24] D. Bag, H. Kour, S. D. Sawant, *Org. Biomol. Chem.* **2020**, *18*, 8278–8293.
[25] C. K. Prier, D. A. Rankic, D. W. C. MacMillan, *Chem. Rev.* **2013**, *113*, 5322–5363.
[26] B. Bartolomei, A. Bogo, F. Amato, G. Ragazzon, M. Prato, *Angew. Chem. Int. Ed.* **2022**, *61*, e202200038.
[27] B. Bartolomei, M. Prato, *Small* **2023**, 2206714.
[28] V. H. Rawal, M. P. Cava, *Tetrahedron Lett.* **1985**, *26*, 6141–6142.
[29] B. Li, R. Li, P. Dorff, J. C. McWilliams, R. M. Guinn, S. M. Guinness, L. Han, K. Wang, S. Yu, *J. Org. Chem.* **2019**, *84*, 4846–4855.
[30] M. Schuler, L. Denosiv, S. Sligar, *Lipid-Protein Interactions: Methods and Protocols*, Springer, New York, **2013**.
[31] F. Arcudi, L. Đorđević, M. Prato, *Angew. Chem. Int. Ed.* **2016**, *55*, 2107–2112.
[32] J. L. Li, T. Y. Liu, Y. C. Chen, *Acc. Chem. Res.* **2012**, *45*, 1491–1500.
[33] D. A. Alonso, A. Baeza, R. Chinchilla, C. Gómez, G. Guillena, I. M. Pastor, D. J. Ramón, *Molecules* **2017**, *22*, 895.
[34] D. M. Fischer, H. Lindner, W. M. Amberg, E. M. Carreira, *J. Am. Chem. Soc.* **2023**, *145*, 774–780.
[35] M. Silvi, P. Melchiorre, *Nature* **2018**, *554*, 41–49.
[36] E. Larionov, M. M. Mastandrea, M. A. Pericas, *ACS Catal.* **2017**, *7*, 7008–7013
[37] A related report uses CNDs to promote the same reaction but employing aerobic conditions relying on a different mechanism: D. Sarma, B. Majumdara, T. K. Sarma, Green Chem. 2019, 21, 6717–6726.

Manuscript received: April 19, 2023
Accepted manuscript online: June 19, 2023
Version of record online: June 28, 2023